DYNAMIC CHARACTERISTICS OF SATURATED DENSE CORAL SAND SAMPLES

Duc Tiep Pham[1,*], Nam Hung Tran[1], Tuong Lai Nguyen[1]

[1]*Institute of Techniques for Special Engineering, Le Quy Don Technical University*

Abstract

Constructions placed on coral sand foundations on offshore islands are often subjected to wave and wind loads which are cyclic dynamic loads. Therefore, a study on the behavior of coral sand under the effect of cyclic dynamic loads is necessary to evaluate the bearing capacity of the structures. This study is devoted to determining dynamic parameters of dense coral sand using Controls dynamic triaxial compression testing device under large deformation and different confining pressure conditions. Parameters analyzed in the present work include excess pore pressure, damping ratio, dynamic elastic modulus and dynamic shear modulus. In addition, to evaluate the correlation between static and dynamic elastic modulus of coral sand, the study conducted additional static triaxial compression experiments according to the consolidated undrained condition. The results showed that an increase in pore water pressure and a decrease in dynamic shear modulus as shear strain increases, while the damping ratio also increases. As the shear strain is less than 0.1%, the damping ratio showed minimal variation. The dynamic elastic modulus of the coral sand is approximately 1.5 times greater than its static elastic modulus.

Keywords: Coral sand; excess pore pressure; damping ratio; dynamic elastic modulus; dynamic shear modulus; confining pressure.

1. Introduction

Vietnam's offshore islands are predominantly formed by coral reefs, consisting of coral sand and coral rock. The coral sand is a significant type of sediment, typically containing very high calcium carbonate content (over 90%) [1]. The coral sand possesses distinct structural characteristics such as angularity, rough surface texture, and irregular particle shapes. As a result, it exhibits specific properties: a high internal friction angle, the presence of apparent cohesion (reflecting interlocking between particles), and the potential for particle breakage under static or dynamic loading conditions [2-4]. Due to these characteristics, coral sand behaves differently from silica sand under both dynamic and static conditions.

Several researchers [5-7] have conducted cyclic triaxial tests in the laboratory on the coral sand under various conditions, revealing that particle breakage due to loading

increases the porosity of coral sand. Under cyclic compression, even at loads lower than the static strength, the coral sand still exhibits significant cumulative deformation. The residual deformation depends on the mean stress applied to the sample (chamber pressure) and the cyclic stress under limiting conditions. Y. Haizhen *et al.* [8] discussed the influence of dynamic stress, confining pressure, consolidation stress ratio, relative density, gradation, and vibration frequency on the dynamic properties of coral through a large number of dynamic triaxial tests. L. Jianguo [9-10], by experimental studies on the dynamic characteristics of saturated coral sand under wave loading, provided a preliminary comparison with the dynamic properties of silica sand. The results indicated that under wave loading, the dynamic strength of both saturated coral sand and silica sand follows a similar variation pattern with the orientation angle of the initial principal stress, and their dynamic strength decreases as the orientation angle of the initial principal stress increases. Coop *et al.* [11] and Donohue *et al.* [12] investigated particle breakage in the coral sand and found that the extent of breakage increases with the duration of cyclic loading.
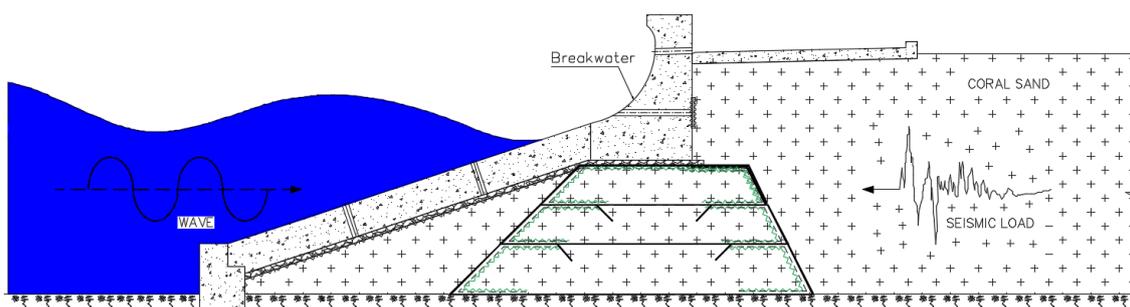

Fig. 1. Dynamic load acting on breakwater.

Research on granular materials under dynamic loading within Vietnam is still limited. Recently, H. N. Nguyen [13] investigated the liquefaction potential of Muong Phang sand from Dien Bien under undrained cyclic loading. D. Nguyen *et al.* [14] studied the dynamic parameters of sand-rubber mixtures with varying proportions through dynamic triaxial testing. Publications specifically addressing the dynamic characteristics of coral sand in Vietnam are particularly scarce, with most studies focusing on its static properties [15-16]. Therefore, in this study, the authors employ a dynamic triaxial apparatus from Controls to examine the dynamic behavior of the saturated coral sand in a dense state under varying confining pressures. Additionally, the authors include a static triaxial test using a consolidated undrained procedure to compare the dynamic and static responses of the coral sand.

2. Determination of dynamic parameters of the saturated coral sand in a dense compacted state by experimental test

2.1. Experimental materials

The coral sand used in this research was sourced from islands in Vietnam sea. The coral sand samples were collected from embankment fill using an open excavation method. For clarity, images illustrating the extraction process of the coral sand are provided in Fig. 2. Although the sampling area lies within the tidal fluctuation zone, experimental results indicate that the embankment fill achieved a dense state due to the compaction effects of construction machinery operating on the islands.

Fig. 2. Progress of using the open excavation method to take coral sand samples and evaluate the compactness.
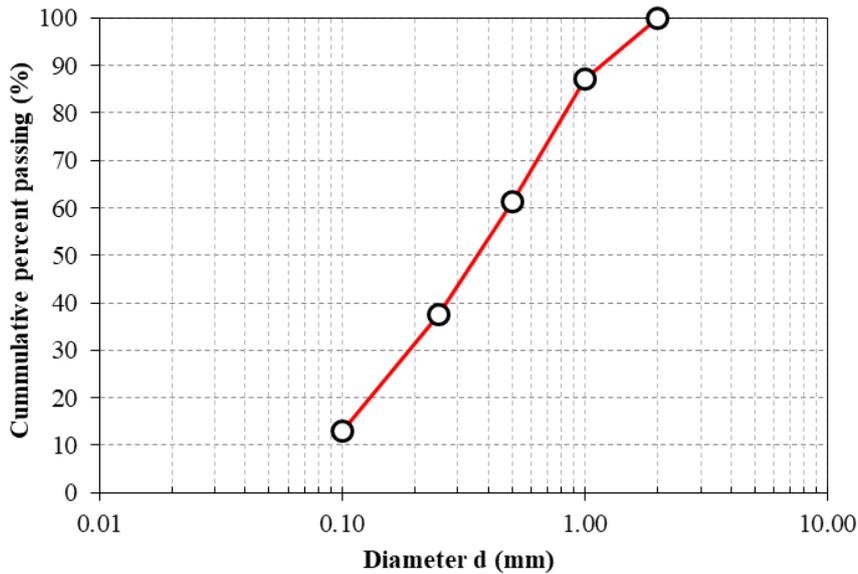

Fig. 3. Grain size distribution curves of coral sand.

The particle-size distribution curves for these coral sands are shown in Fig. 3 and the physical properties of the studied materials are shown in Table 1. The particle-size distribution curve reveals a coefficient of uniformity (C_u) of 6.31 and a coefficient of curvature (C_c) of 1.11.

Table 1. Physical properties of coral sand

Soil Properties	Value
Specific gravity, G_s	2.671
Maximum void ratio, e_{max}	0.927
Minimum void ratio, e_{min}	0.600
Coefficient of uniformity, C_u	6.31
Coefficient of curvature, C_c	1.11

2.2. Overview of the experimental procedure

In this study, we prepared three cylindrical test specimens, with a specimen diameter of $D = 70$ mm and a specimen height of $H = 140$ mm, and achieved a relative density of $D_r = 70\%$. In order to control the uniformity of material density in the samples, the coral sand was divided into 4 layers and they were compacted layer by layer during each sample preparation. Each layer was compacted wet, ensuring that the thickness of each compacted layer was a multiple of $H/4 = 35$ mm. The sample was subjected to CO_2 flushing for 30 minutes (Fig. 5). CO_2 gas, having a higher density than the air within the sample, displaces the trapped air, thus removing it from the specimen. After the CO_2 flushing, the pore spaces were nearly completely filled with CO_2, and then de-aerated water was passed through the specimen. The water dissolved the CO_2, leaving the pores entirely filled with water. The main experimental procedure followed these stages:

Saturation stage: The sample was saturated by adjusting the chamber pressure and back pressure. The saturation process was deemed complete when the saturation coefficient $B \geq 0.95$.

Consolidation stage: The chamber pressure and back pressure were adjusted to achieve the desired effective confining pressures ($\sigma_3' = 100;\ 200;\ 300$ kPa). Consolidation was considered complete once the excess pore water pressure had dissipated to match the back pressure.

- Dynamic loading stage: Dynamic loading was applied according to ASTM D3999 [17]. A sinusoidal load was applied on the top of the specimen at a frequency of $f = 0.1$ Hz, with the cyclic stress ratio (CSR) varying from 0.1 to 0.3.
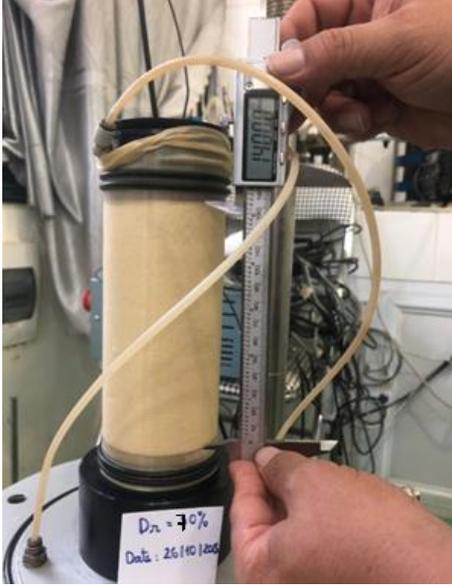

Fig. 4. Sample after preparation.

Fig. 5. Perform CO_2 aeration into the sample.

Figure 6 presents the stress-strain characteristics of the soil under cyclic axial loading. The shear modulus G and damping ratio D were automatically calculated and recorded according to ASTM D3999 [17], as follows:

- Dynamic shear strain in the sample:

$$\gamma_{SA} = \frac{\varepsilon_{SA}}{1+\upsilon} \cdot 100\% \tag{1}$$

where γ_{SA} is dynamic shear strain, $\varepsilon_{SA} = \dfrac{\varepsilon_{DA}}{2}$ is single amplitude axial strain, $\varepsilon_{DA} = \dfrac{S_{DA}}{L_S}$ is double amplitude axial strain, υ is Poisson's ratio, S_{DA} is double amplitude displacement (mm), L_S is the height of the sample after consolidation (mm).

- The dynamic modulus of elasticity is calculated as follows:

$$E = \frac{L_{DA}}{S_{DA}} \cdot \frac{L_S}{A} \tag{2}$$

where L_{DA} is double amplitude load, A is cross-section area of the sample.

98

- The dynamic shear modulus of a specimen is determined as follows:

$$G = \frac{E}{2(1+\upsilon)} \tag{3}$$

The damping ratio is a critical dynamic parameter of soil that represents the hysteretic behavior of the stress-strain relationship under cyclic loading. It also reflects energy dissipation. The damping ratio D can be determined using the following formula:

$$D = \frac{A_L}{4\pi \cdot A_T} \cdot 100\% \tag{4}$$

in which A_L is an area within the hysteresis loop (kN.m), $A_T = 0.5 \cdot L \cdot S$.
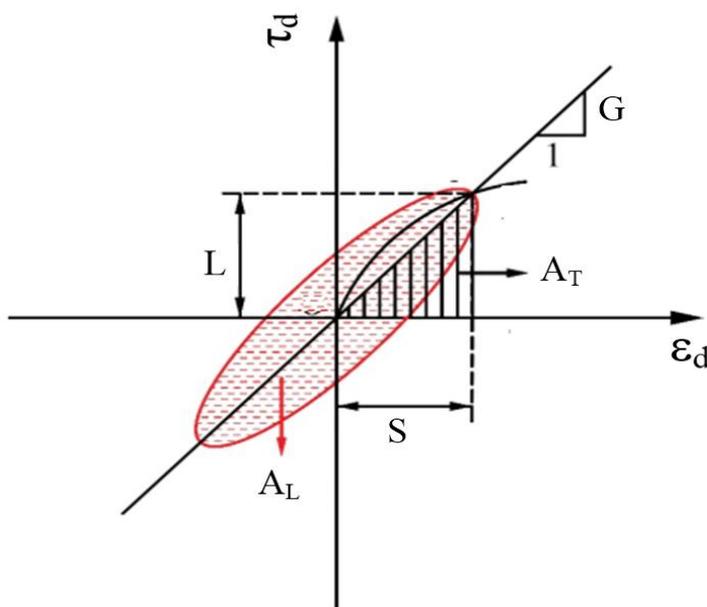
Fig. 6. Graph for determining the dynamic shear modulus and damping ratio of coral sand.

2.3. Results of dynamic triaxial testing and discussion

The results of the dynamic triaxial tests conducted on coral sand specimens under various confining pressures are presented from Fig. 7 to Fig. 10. Observations from these figures allow for the following conclusions:

In the undrained condition, under the influence of cyclic loading, the shear strain increases, and the excess pore water pressure also rises (Fig. 7). The increase in excess pore water pressure reduces the shear strength of coral sand (as pore pressure increases,

effective stress decreases) and consequently reduces stiffness (Fig. 8 and 9). As stiffness decreases, the coral sand specimen becomes softer, leading to an increase in the damping ratio (Fig. 10).

- The moment at which the specimens reach failure corresponds with the peak excess pore water pressure and damping ratio, as well as the stiffness decreasing to zero.

- A higher confining pressure results in greater pore pressure, an increased dynamic modulus of elasticity (or dynamic shear modulus), and a lower damping ratio.

- When the shear strain is less than 0.1%, the damping ratio exhibits minimal variation. At a confining pressure of $\sigma_3 = 100$ kPa, $D = (4$-$8)\%$; at $\sigma_3 = 150$ kPa, $D = (4$-$6)\%$; and at $\sigma_3 = 200$ kPa, $D = (2$-$3)\%$.

- A comparison of the dynamic parameters of silica sand [14] and coral sand reveals that, for similar conditions, coral sand possesses a greater stiffness (shear modulus) than silica sand, while the damping ratio of coral sand is lower than that of silica sand. Within the range of shear strains less than 0.1%, the damping ratio changes linearly with the increase in shear strain, whereas for coral sand, the damping ratio varies very little.
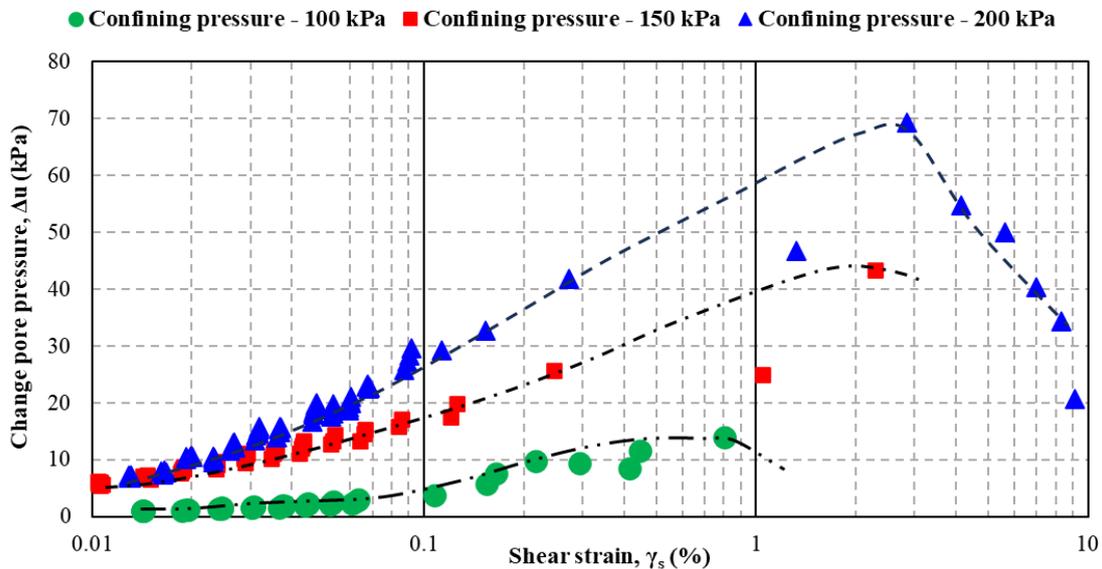

Fig. 7. Correlation between shear strain and changes in pore water pressure under different confining pressures.
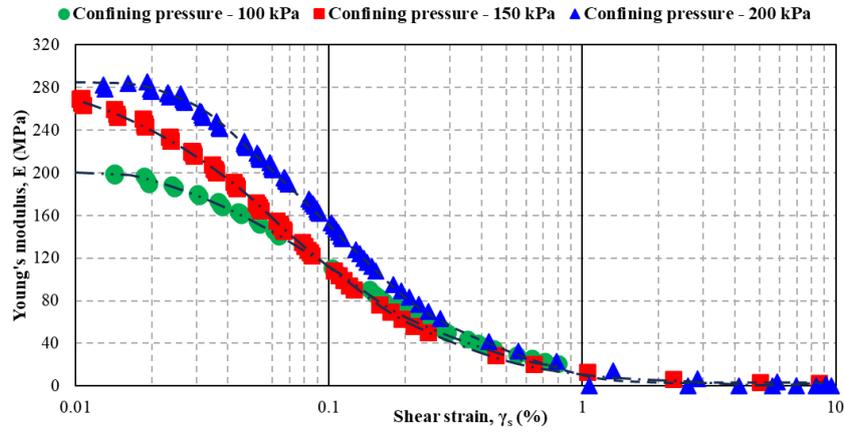
Fig. 8. Correlation between shear strain and elastic modulus under different confining pressures.
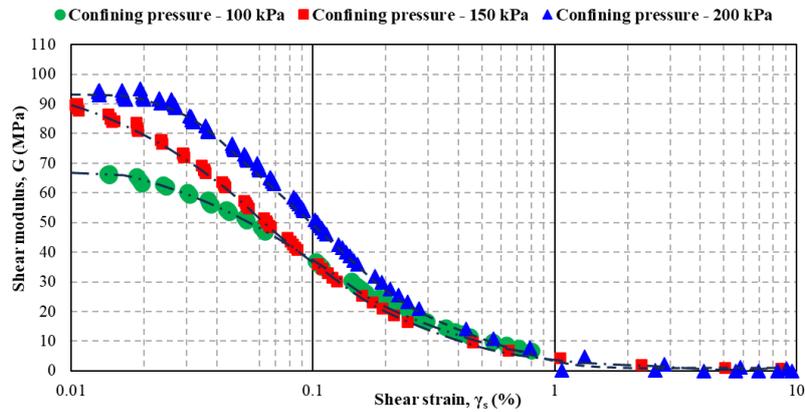

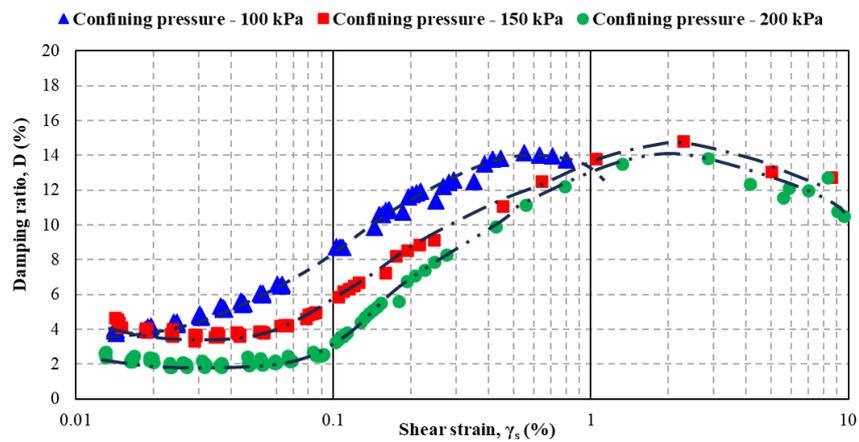*Fig. 9. Correlation between shear strain and shear modulus under different confining pressures.*

Fig. 10. Correlation between shear strain and damping ratio under different confining pressures.

101

3. Experimental study to determine the static elastic modulus of dense coral sand

Some authors, when modeling the interaction between structures and soil subjected to seismic loading [18], still utilize soil parameters derived from conventional static tests (such as unconfined compression, consolidation, and static triaxial tests). However, research by Xiaolan Liu and colleagues [19] indicated that the dynamic elastic modulus is 1.8 to 2.3 times greater than the static elastic modulus under similar conditions (moisture, density, and confining pressure). Therefore, in this study, the authors conduct additional static triaxial tests to investigate the behavior of the coral sand under static loading and to compare the values of the modulus of elasticity of coral sand under both dynamic and static loads. For this test, we used a cylindrical sample of the same size as the dynamic tests, i.e., the sample diameter is 70mm and the sample height is 140mm.

The procedure for conducting static triaxial tests on the coral sand samples follows a similar approach to that of dynamic triaxial tests (with a sample density of D_r = 70% and confining pressure σ_3 = 100 kPa). After the sample completes the isotropic consolidation process, static loading is applied. The results of the experiments are presented in Fig. 11. It can be observed that the curve depicting the relationship between axial strain and stress deviation reaches a peak value at approximately 8.5% strain, after which it tends to stabilize. This behavior indicates that the coral sand sample adheres to the principles of the Hardening Soil (HS) or Hypoplastic models.
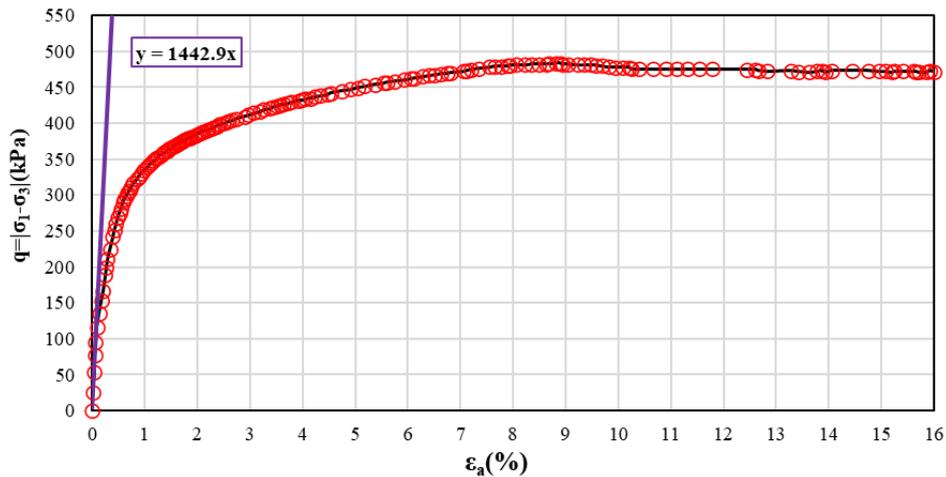

Fig. 11. Correlation between axial strain and stress deviation during the static compression of the sample under consolidated undrained (CU) conditions (confining pressure σ_3 = 100 kPa).

Based on the correlation between axial strain and stress deviation during the static compression of the coral sand samples under consolidated undrained conditions, the static elasticity modulus of the coral sand can be determined, $E_0 = 144.29$ MPa. Comparing the dynamic experimental results with the static ones shows the correlation between the dynamic elastic modulus and the static elastic modulus. Specifically, in this study the dynamic elasticity modulus of the coral sand is approximately 1.5 times greater than the static elasticity modulus (210.5 MPa/144.29 MPa = 1.459).

4. Conclusion

In this study, the authors conducted dynamic triaxial tests on coral sand samples collected from offshore islands in Vietnam. The samples were prepared in a dense state, reflecting the current conditions of the engineered fill based on field assessments. The research findings indicate:

Saturated coral sand samples subjected to cyclic loading under undrained conditions exhibit an increase in pore water pressure and a decrease in dynamic shear modulus as shear strain increases, while the damping ratio also increases.

When the shear strain is less than 0.1%, the damping ratio shows minimal variation.

The dynamic modulus of the Hong River [14] sand is lower than that of the coral sand under the same conditions (confining pressure and relative density), whereas the damping ratio of the Hong River sand is greater than that of the coral sand.

Within the range of shear strains less than 0.1%, the damping ratio of the Hong River sand varies linearly with increasing shear strain, while the damping ratio of coral sand shows little variation.

Within the number of samples in this study, the experimental results showed that the dynamic elasticity modulus of the coral sand is approximately 1.5 times greater than the static elasticity modulus.

Acknowledgement

References

[1]   W. Ma, Y. Qin, Q. Wu, G. Zhang, and G. Chen, "Cyclic failure mechanisms of saturated marine coral sand under various consolidations", *Applied Ocean Research*, Vol. 131, 2023, 103450. DOI: 10.1016/j.apor.2022.103450

[2]   M. R. Coop, "The mechanics of uncemented carbonate sands", *Géotechnique*, Vol. 40, Iss. 4, pp. 607-626, 1990. DOI: 10.1680/geot.1990.40.4.607

[3]   R. Gao and J. Ye, "Mechanical behaviors of coral sand and relationship between particle breakage and plastic work", *Engineering Geology*, Vol. 316, 2023, 107063. DOI: 10.1016/j.enggeo.2023.107063

[4]   Z. Wang and L. Zhang, "Experimental study on dynamic parameters of calcareous sand subgrade under long-term cyclic loading", *Journal of Marine Science and Engineering*, Vol. 10, Iss. 12, 2022, 1806. DOI: 10.3390/jmse10121806

[5]   M. Datta, G. V. Rao, and S. Gulhati, "Development of pore water in a dense calcareous sand under repeated compressive stress cydes", in *Proceedings of the International Symposium on Soils under Cyclic and Transient Loading*, Suansea, Wales, UK, 7-11 January 1980, pp. 33-47.

[6]   K. Knight, "Contribution to the performance of calcareous sands under cyclic loading", in *Proceedings of the International Conference on Calcareous Sediments*, Perth, WA, Australia, 15-18 March 1988, pp. 877-880.

[7]   W. S. Kaggwa, H. G. Poulos, and J. P. Carter, "Response of carbonate sediments under cyclic triaxial test conditions", in *Proceeding of the 1st International Conference on Calcareous Sediments*, Perth, WA, Australia, 15-18 March 1988, Vol. 1, pp. 97-107.

[8]   Y. Haizhen and W. Ren, "The cyclic strength test research on calcareous sand", *Rock and Soil Mechanics*, Vol. 4, pp. 3-5, 1999 (in Chinese).

[9]   L. Jianguo, W. Ren, and Y. Haizhen, "Experimental research on effect of initial principal stress orientation on dynamic properties of calcareous sand", *Rock and Soil Mechanics*, Vol. 5, pp. 723-727, 2005 (in Chinese).

[10]   J. G. Li, "Experimental research on dynamic behavior of saturated calcareous sand under wave loading", Ph.D. thesis, Institute of Rock and Soil Mechanics, Chinese Academy of Sciences, 2005.

[11]   M. R. Coop, K. K. Sorensen, T. M. Bodas Freitas, and G. Georgoutsos, "Particle breakage during shearing of a carbonate sand", *Géotechnique*, Vol. 54, pp. 157-163, 2004.

[12]   S. Donohue, C. O'Sullivan, and M. Long, "Particle breakage during cyclic triaxial loading of a carbonate sand", *Géotechnique*, Vol. 59, pp. 477-482, 2009. DOI: 10.1680/geot.2008.T.003

[13]   N. H. Nam, N. C. Linh và Đ. S. Mai, "Nghiên cứu hóa lỏng cát Mường Phăng, Điện Biên chịu tải trọng chu kỳ không thoát nước", *Tạp chí Khoa học và Công nghệ Việt Nam*, Tập 58, Số 7, tr. 24-27, 2016.

[14]   H. Đ. Nguyên, V. V. Tuấn và P. Đ. Tiệp, "Nghiên cứu tham số động của hỗn hợp cát cao su với tỷ lệ khác nhau bằng thí nghiệm nén ba trục động", *Tạp chí Vật liệu và Xây dựng - Bộ Xây dựng*, Vol. 12, No. 03, 2022. DOI: 10.54772/jomc.03.2022.306

[15]   P. Đ. Tiệp, N. T. Lai và V. A. Tuấn, "Nghiên cứu thực nghiệm xác định các tham số chống cắt của cát san hô bằng máy cắt phẳng tự động", *Journal of Science and Technique - Section on Special Construction Engineering*, Vol. 2, No. 02, 2019. DOI: 10.56651/lqdtu.jst.v2.n02.225.sce

[16] C. V. Hoa, V. A. Tuan, N. T. Sang, N. T. Lai, and P. D. Tiep, "Effect of grain size on Shear Strength of Coral Gravel Sand", in *Proceedings of the 3rd International Conference on Sustainability in Civil Engineering: ICSCE 2020*, 26-27 November, Hanoi, Vietnam, 2021, pp. 87-95, Springer Singapore. DOI: 10.1007/978-981-16-0053-1_11

[17] ASTM D3999. Standard Test Methods for the Determination of the Modulus and Damping Properties of Soils Using the Cyclic Triaxial Apparatus.

[18] N. A. Vu, C. Q. Cao, and V. H. Nguyen, "Calculation of tunnel linings under seismic loads of the earthquakes by generated the artificial acceleration applied in the Ha Noi area", *Journal of Science and Technique-Section on Special Construction Engineering*, Vol. 3, No. 01, pp. 81-93, 2020. DOI: 10.56651/lqdtu.jst.v3.n01.75.sce

[19] X. Liu, X. Zhang, H. Wang, and B. Jiang, "Laboratory testing and analysis of dynamic and static resilient modulus of subgrade soil under various influencing factors", *Construction and Building Materials*, Vol. 195, pp. 178-186, 2019. DOI: 10.1016/j.conbuildmat.2018.11.061

NGHIÊN CỨU ĐẶC TRƯNG ĐỘNG
CỦA MẪU CÁT SAN HÔ BÃO HÒA Ở TRẠNG THÁI CHẶT

Phạm Đức Tiệp[1], Trần Nam Hưng[1], Nguyễn Tương Lai[1]

[1]*Viện Kỹ thuật công trình đặc biệt, Trường Đại học Kỹ thuật Lê Quý Đôn*

Tóm tắt: Các công trình ở các đảo xa bờ thường xuyên chịu tác dụng của tải trọng sóng-gió, đây là loại tải trọng động có tính chu kỳ. Do đó, cần nghiên cứu về ứng xử của cát san hô dưới tác động của tải trọng động chu kỳ để đánh giá khả năng chịu lực của các công trình. Nghiên cứu này tiến hành xác định các tham số động của cát san hô ở trạng thái chặt bằng thiết bị thí nghiệm 3 trục động Controls dưới điều kiện biến dạng lớn và áp lực buồng khác nhau. Các tham số được phân tích trong nghiên cứu như áp lực lỗ rỗng dư, tỉ số cản, mô đun đàn hồi và mô đun trượt động. Đồng thời, để đánh giá mối tương quan giữa mô đun đàn hồi tĩnh và động của cát san hô, các tác giả đã tiến hành bổ sung thí nghiệm 3 trục tĩnh theo sơ đồ cố kết - không thoát nước. Kết quả cho thấy áp lực nước lỗ rỗng tăng và mô đun cắt động giảm khi biến dạng cắt tăng, trong khi hệ số giảm chấn cũng tăng. Khi biến dạng cắt nhỏ hơn 0,1%, tỉ lệ giảm chấn thay đổi không nhiều. Mô đun đàn hồi động của cát san hô lớn hơn mô đun đàn hồi tĩnh của nó khoảng 1,5 lần.

Từ khóa: *Cát san hô; áp lực lỗ rỗng dư; tỉ số cản; mô đun đàn hồi động; mô đun trượt động; áp lực buồng.*

❑